UC San Diego

UC San Diego Electronic Theses and Dissertations

Title

The protective role of S-nitrosoglutathione reductase (GSNOR) against excessive NO-dependent S-nitrosylation of myofibrillar and/or Ca2+-handling proteins in mouse fast-twitch skeletal muscle during fatigue and recovery

Permalink

https://escholarship.org/uc/item/00t2k2rx

Author

Gilmore, Natalie Kori

Publication Date

2021

Peer reviewed|Thesis/dissertation

eScholarship.org Powered by the California Digital Library
University of California

UNIVERSITY OF CALIFORNIA SAN DIEGO

The protective role of S-nitrosoglutathione reductase (GSNOR) against excessive NO-dependent S-nitrosylation of myofibrillar and/or Ca^{2+}-handling proteins in mouse fast-twitch skeletal muscle during fatigue and recovery

A thesis submitted in partial satisfaction of the
requirements for the degree of Master of Science

in

Biology

by

Natalie Kori Gilmore

Committee in charge:

Professor Michael C. Hogan, Chair
Professor Shelley Halpain, Co-Chair
Professor Milton Saier

2021

Copyright

Natalie Kori Gilmore, 2021
All rights reserved.

The thesis of Natalie Kori Gilmore is approved, and it is acceptable in quality and form for publication on microfilm and electronically.

University of California San Diego

2021

TABLE OF CONTENTS

THESIS APPROVAL PAGE ... iii
LIST OF FIGURES ... v
LIST OF ILLUSTRATIONS ... vi
LIST OF ABBREVIATIONS ... vii
ACKNOWLEDGEMENTS ... ix
ABSTRACT OF THE THESIS ... x
HYPOTHESIS ... 1
AIMS ... 2
INTRODUCTION ... 3
METHODS ... 9
DISCUSSION ... 24
REFERENCES ... 31

LIST OF FIGURES

Figure 1. EDL Protocol #1: Force-frequency curves from EDL muscles before and after 20 min incubation with either $GSNOR_i$ (10 μM; FF#2) incubation or untreated. 15

Figure 2. EDL Protocol #1: Force development during repetitive contractions evoked by 100 Hz stimulations each 3 seconds (0.33 tps) for 2 min. 17

Figure 3. EDL Protocol #2: Time course of force recovery after EDL Fatigue Protocol #2 at submaximal (30 and 50 Hz) and maximal (120 Hz) frequencies of stimulation. 18

Figure 4. Effects of $GSNOR_i$ + L-NMMA incubation before and after EDL Fatigue Protocol #2. 19

Figure 5. Percentage of force evoked by each frequency of stimulation 30 min after Fatigue #1 (A) and Fatigue #2 (B) compared to pre-fatigue force development in the single myofiber protocol. 20

Figure 6. Cytosolic Ca^{2+} concentration ($[Ca^{2+}]_c$) measured during FF protocols before and 30 min after a fatigue bout before treatments (A) and after treatment with either 10 μM $GSNOR_i$ (n=5) or DMSO (vehicle) in FDB myofibers (n=4) (B). 21

Figure 7. Mean data showing the $[Ca^{2+}]_c$-Force relationship for DMSO (n=4) (A) and $GSNOR_i$ (n=5) (B) treated myofibers. 22

Figure 8. Mean time to fatigue for myofibers in Fatigue #1 (no treatment) vs. Fatigue #2 (($GSNOR_i$) (n=5) or DMSO treatment (n=4)). 23

LIST OF ILLUSTRATIONS

Illustration 1. During repetitive contractions, we hypothesize that blocking GSNOR will lead to a buildup of GSNO, which will then modify myofibrillar and/or Ca^{2+}-handling proteins. 1

Illustration 2. Scheme of the intact EDL muscle system used in this study. 10

Illustration 3. Scheme of EDL Protocol #1. 11

Illustration 4. Scheme of EDL Protocol #2. 12

Illustration 5. Scheme of FDB single myofiber protocol. 14

Illustration 6. Scheme of experimental setup for the FDB single myofiber protocol. 14

LIST OF ABBREVIATIONS

Acetyl CoA = acetyl coenzyme A

AP = action potential

ADH = alcohol dehydrogenase

ADP = adenosine diphosphate

AMP = adenosine monophosphate

ATP = adenosine triphosphate

β = ratio of fluorescence between high and no $[Ca^{2+}]_c$ at 380 nm

$[Ca^{2+}]_c$ = cytosolic Ca^{2+} concentration

CFS = chronic fatigue syndrome

COPD = chronic obstructive pulmonary disease

CSA = cross-sectional area

DHPR = dihydropyridine receptor; L-type Ca^{2+} channel

DMSO = dimethyl sulfide

EDL = extensor digitorum longus muscle

eNOS = endothelial nitric oxide synthase

FADH = reduced flavin adenine dinucleotide

FDB = flexor digitorum brevis muscle

FF = force-frequency

FURA-2 = pentapotassium Salt, cell impermeant; a fluorescent dye that binds to intracellular Ca^{2+}

GSH = reduced glutathione

GSNO = S-nitrosoglutathione

GSNOR = S-nitrosoglutathione reductase

$GSNOR_i$ = GSNOR inhibitor

Hz = Hertz; s-1

IMP = inosine monophosphate

iNOS = inducible nitric oxide synthase

K_D = dissociation constant

kPa = kilopascal

L-NMMA = NG-Methyl-L-arginine acetate salt; a NOS inhibitor

L_0 = maximal isometric twitch force

mN = millinewton

MHC = myosin heavy chain

NADH = reduced nicotinamide adenine dinucleotide

NMJ = neuromuscular junction

nNOS = neuronal nitric oxide synthase

NO = nitric oxide

NOS = NO synthase

NO = $NO^{\bullet}$; nitric oxide

PLFFD = prolonged low frequency force depression

R = ratio of fluorescence excitation

R_{max} = the fluorescence ratio found at high $[Ca^{2+}]_c$ when binding is maximal

R_{min} = the fluorescence ratio at low $[Ca^{2+}]_c$ when Ca^{2+}-FURA-2 binding is minimal

RYR = ryanodine receptor

-SH = sulfhydryl group

SNAP = S-nitroso-N-acetylpenicillamine; an NO donor

SNO-RAC = S-nitrosothiol-resin assisted capture

SR = sarcoplasmic reticulum

TCA cycle = tricarboxylic acid cycle; Kreb's cycle

tps = trains per second

ACKNOWLEDGEMENTS

I would like to acknowledge Professor Michael C. Hogan for his support as the chair of my committee. Not only has Mike been a mentor to me in the laboratory, but he has also been someone that I have looked up to for career and life advice. After I joined the Hogan Lab as an undergraduate, I discovered that Mike happened to be a pole vaulter, just like me. He inspired me to get into coaching, and I hope that someday I'll be half as good of a coach as he is.

I would like to express my deep gratitude for Dr. Leonardo Nogueira, my research advisor, for giving me this research project and for teaching me about muscle physiology. Leo is deeply knowledgeable in this field and he has taught me all the techniques I performed in this research project. He was my first laboratory mentor and I'm grateful that I was able to learn so much from him.

I would also like to thank Professor Shelley Halpain for agreeing to be my thesis committee co-chair. I took her course The Healthy and Diseased Brain and then later had the pleasure of being a Teaching Assistant for the same course. Her passion for science and dedication to educating students is evident and she was one of the most memorable aspects of my education at UCSD.

I would like to thank Professor Milton Saier for kindly agreeing to be on my thesis committee. His suggestions and review of my thesis are greatly appreciated.

To everyone I've met and worked with in my time as a student in the Division of Physiology, thank you for your support and for being such a great little research community at UCSD. I would like to thank Janelle Fine for always helping us fix our equipment; my experiments would not have run so smoothly without her engineering talents. I would like to thank Dr. Esteban Moya Cespedes for always taking time to help me and answer any questions I had. Thank you to Professor Daniel Cannon from SDSU, Dr. Ellen Breen, and Dr. Yoshitake Cho for being great sources of knowledge and for letting me participate in collaborations. Most of all, thank you to Cynthia Indralingam for being the best friend I could ask for – I'm so glad we were able to meet through research and do the Master's program together.

Material from this thesis is being prepared for submission for publication. The thesis author was the author of the material. Leonardo Nogueira and Michael C. Hogan were co-authors of the material.

ABSTRACT OF THE THESIS

The protective role of S-nitrosoglutathione reductase (GSNOR) against excessive NO-dependent S-nitrosylation of myofibrillar and/or Ca^{2+}-handling proteins in mouse fast-twitch skeletal muscle during fatigue and recovery

by

Natalie Kori Gilmore

Master of Science in Biology

University of California San Diego, 2021

Professor Michael C. Hogan, Chair
Professor Shelley Halpain, Co-Chair

Skeletal muscle fibers produce nitric oxide (NO) and possibly the S-nitrosylated form of glutathione, S-nitrosoglutathione (GSNO), due to Ca^{2+} transients during fatigue. GSNO reductase (GSNOR), an enzyme that denitrosylates S-nitrosothiols, scavenges GSNO to protect proteins from being S-nitrosylated. Prior studies have revealed GSNOR as a protective enzyme against excessive S-nitrosylation by GSNO in many tissues, but it has not been shown to directly regulate proteins during fatigue in skeletal

muscle. We investigated the role of GSNOR during fatiguing contractions, particularly the acute effects of a pharmacological GSNOR inhibitor ($GSNOR_i$), on fast-twitch muscle contractility and fatigue resistance using whole extensor digitorum longus (EDL) muscles and intact single flexor digitorum brevis (FDB) myofibers from mice. $GSNOR_i$ did not result in any changes in contractile function under non-fatiguing conditions. EDL exposed to $GSNOR_i$ were less fatigue tolerant and less capable of recovering after fatigue. NO synthase (NOS) inhibitor NG-Methyl-L-arginine (L-NMMA) blocked $GSNOR_i$'s effects on fatigue tolerance and recovery. $GSNOR_i$ treated myofibers exhibited depressed recovery of contractile force post-fatigue compared to controls treated with dimethyl sulfoxide (DMSO), the vehicle used to solubilize $GSNOR_i$, matching the EDL data. Myofibers showed no changes in Ca^{2+}-handling or the force-Ca^{2+} relationship, nor in time to fatigue, thereby contradicting the results of our EDL experiments. These data suggest that NO produced during muscle fatigue leads to an increase in GSNO, which may subsequently lead to an increase in intracellular S-nitrosothiols that specifically alters myofibrillar rather than Ca^{2+}-handling protein function, and that GSNOR regulates against excessive S-nitrosylation of these proteins.

HYPOTHESIS

This study will test the hypothesis that increased nitric oxide production during fatiguing contractions causes increased levels of S-nitrosoglutathione (GSNO) in fast-twitch skeletal muscle, and that the enzyme GSNO reductase (GSNOR) degrades GSNO to curb excess S-nitrosylation of myofibrillar and/or Ca^{2+}-handling proteins by GSNO, thereby preventing modifications that are detrimental to muscle force production during fatigue and recovery.

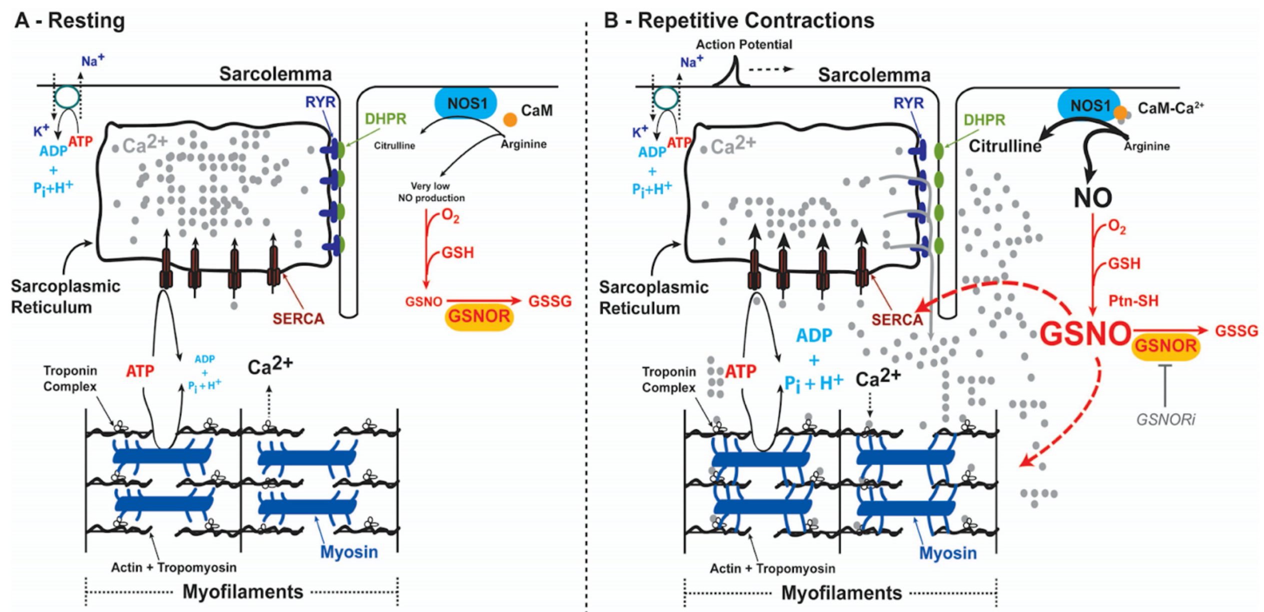

Illustration 1. During repetitive contractions, we hypothesize that blocking GSNOR will lead to a buildup of GSNO, which will then modify myofibrillar and/or Ca^{2+}-handling proteins.

AIMS

1. To investigate the effects of acute GSNOR inhibition in intact skeletal muscle contractility ex-vivo during and after fatiguing contractions.
2. To investigate whether inhibition of GSNOR alters post-fatigue force and/or Ca^{2+}-handling in intact single myofibers.

INTRODUCTION

Recovery of contractile force of skeletal muscles after fatigue is essential to regaining full muscle capacity after strenuous activity. Skeletal muscle fatigue can be defined broadly as the decrease in maximal contractile force in response to contractile activity (Wan *et al.,* 2017). Ultimately, muscle fatigue is the culmination of several cellular processes that occur after the initiation of intense activity and result in a reduction in the muscle's ability to generate force and power, which can last days or even up to a few weeks (Green, 1997). Fatigue can be difficult to study in vivo because it is simultaneously under central and peripheral control and the fatigue may occur at any point in the excitation-contraction coupling process (Allen *et al.,* 2008). Therefore, several methods have been developed to isolate specific mechanisms that may contribute to fatigue; our research follows two general fatigue models: isolated muscle, and isolated single myofiber.

While fatigue always occurs following activity that is sufficiently intense, fatigue tolerance can be modified by several factors. If muscle is unable to completely recover after a single or many fatiguing events, a number of health concerns including overwork, chronic fatigue syndrome (CFS), and overtraining syndrome may result. Fatigue resistance is the ability of the muscle to preserve force production under fatiguing conditions. The major factor that determines fatigue resistance of a myofiber is its oxidative capacity and density of mitochondria (Allen *et al.,* 2008). Incomplete recovery from fatigue is also a symptom associated with a number of diseases (Wan *et al.,* 2017). Understanding the biochemical mechanisms underlying skeletal muscle fatigue and recovery is of great interest to athletes ranging from amateur to professional, to coaches, and to exercise physiologists because of its potential to uncover ways to reduce the time and severity of muscle fatigue. Mechanisms that underlie fatigue may also be important for understanding the bases of syndromes and diseases that involve exercise intolerance. Patients with chronic obstructive pulmonary disorder (COPD) often exhibit exercise intolerance and complain of dyspnea on exertion (Kim *et al.,* 2008). Both Type 1 and Type 2 diabetic patients commonly develop myopathy, with associated changes in skeletal muscle metabolism, muscle atrophy, decreased capillary density, and an increase in the number of glycolytic fibers (D'Souza *et al.,* 2013), all of which result in impaired skeletal

muscle strength and exercise tolerance. There is also evidence suggesting exercise intolerance in heart failure patients is caused by impaired skeletal muscle fatigue tolerance, rather than solely due to cardiac dysfunction (Keller-Ross *et al.,* 2019). Uncovering the mechanisms underlying muscle fatigue may be useful in developing treatments to improve the quality of life of patients with these conditions, as well as potentially leading to finding ways to help athletes avoid the prolonged effects of post-exercise fatigue.

Muscle contractility is triggered by the depolarization of the muscle fiber membrane, also known as the sarcolemma, and activation of the myofilaments following the release of acetylcholine at the neuromuscular junction (NMJ) by the motor neuron. This process has been named excitation-contraction coupling (Allen *et al.,* 2008). It links the arrival of a nerve action potential (AP) of the presynaptic motor neuron at the NMJ with the release of acetylcholine, and binding of acetylcholine to nicotinic receptors on the sarcolemma, followed by a wave of membrane depolarization of the postsynaptic myofiber. The depolarization of the membrane initiates a muscle AP; from there, the muscle AP is conducted quickly and bidirectionally along the sarcolemma and then more slowly down t-tubules (Allen *et al.,* 2008) to reach the inner portions of the muscle fiber, where it triggers a conformational change in voltage-gated L-type Ca^{2+} channels (dihydropyridine receptors; or DHPRs), which in turn triggers the opening of ryanodine receptors (RYRs), present in the membrane of the sarcoplasmic reticulum (SR) (Allen *et al.,* 2008). Opening of RYR leads to rapid Ca^{2+} diffusion from the SR to the cytosol. Ca^{2+} released into the sarcoplasm is necessary for muscle contraction to begin according to the sliding filament theory.

After stimulation by their motor neurons, skeletal muscles generate force according to the heavily studied sliding filament theory, which involves two filaments of fixed length shortening the length of the muscle as they slide toward each other (Cooke, 2004). The structural unit of skeletal muscle is the sarcomere, which contains overlapping arrays of filaments, actin and myosin, (Squire, 2016) that repeat along the length of the muscle. Actin contains sites where myosin, or the thick filament, can bind; the complex containing actin, the troponin complex, and tropomyosin is called the thin filament. The troponin complex (composed of troponin C, troponin I, and troponin T) is bound to tropomyosin at rest, but the binding of Ca^{2+}, released during a muscle action potential, to troponin C causes a conformational change

that moves tropomyosin away from the myosin binding site of actin and allows myosin initiate the cross-bridge cycle (Mukund & Subramaniam, 2020). Myosin has a neck region that acts as a lever arm powered by adenosine triphosphate (ATP) hydrolysis, which shortens the sarcomere when the neck changes its orientation to produce a power stroke before it detaches (Cooke, 2004).

The cellular processes that underlie contraction, including regulation of intracellular Ca^{2+} handling and crossbridge cycling, must be greatly accelerated during intense and fatiguing activity (Green, 1997) because the muscle's rate of ATP use is up to 1,000 times higher than at rest (Baker *et al.,* 2010). Skeletal muscle relies on three systems to supply ATP: phosphagen, glycolytic, and mitochondrial respiration; all three systems contribute (but at different percentages) according to the intensity and duration of exercise (Baker *et al.,* 2010).

The phosphagen system is composed of three reactions catalyzed by creatine kinase: 1) resynthesize ATP from creatine phosphate and adenosine diphosphate (ADP) by phosphate exchange; 2) adenylate kinase, which combines two ADP molecules to form ATP and adenosine monophosphate (AMP); and 3) AMP deaminase, which converts AMP and a proton into inosine monophosphate (IMP) and NH_4^+. The first two reactions regenerate ATP and produce AMP, the latter of which is a strong allosteric activator of key glycolytic enzymes (Baker *et al.,* 2010). The phosphagen system is rapidly activated upon contractile activity, but also is quickly depleted. It is commonly accepted that the phosphagen system is responsible for nearly all the ATP production in skeletal muscle for the first 5-6 seconds of intense exercise (Baker *et al.,* 2010).

The second system, glycolysis, is rapidly activated in exercising muscle by high AMP and it utilizes both blood glucose and muscle glycogen stores to form pyruvate. Glycolysis starts producing a small ATP yield almost immediately following onset of intense exercise but reaches its maximal rate of ATP regeneration at around 10-15 seconds and can maintain high levels of ATP regeneration for longer (2-3 min in a trained athlete) than the phosphagen system (Baker *et al.,* 2010). One molecule of glucose only produces net 2 ATP molecules during glycolysis (Melkonian & Schury, 2020).

The third system, mitochondrial respiration, has a high oxidative capacity and energy efficiency and is best suited to sustain prolonged work (Zoll *et al.,* 2002). This system involves an oxygen-dependent pathway that uses pyruvate and reduced nicotinamide adenine dinucleotide (NADH) created from glycolysis as substrates – so that for each molecule of glucose that enters the pathway, up to 32 ATP molecules can be produced (Melkonian & Schury, 2020). Another reaction pathway that occurs is *β*-oxidation, which occurs in the mitochondria and degrades saturated fatty acids two carbons at a time resulting in production of acetyl coenzyme A (acetyl CoA) (which may then enter the tricarboxylic acid (TCA) cycle and contribute to mitochondrial respiration) as well as NADH and reduced flavin adenine dinucleotide (FADH) (Baker *et al.,* 2010). ATP turnover from mitochondrial respiration is initiated at approximately 10 seconds following the onset of exercise (Gandra *et al.,* 2012) and ramps up over the first 100 seconds following the onset of exercise (Baker *et al.,* 2010). Although full oxidative phosphorylation is much more energy efficient at producing ATP than anaerobic glycolysis, it is actually approximately a hundred times slower than glycolysis (Melkonian & Schury, 2020) and is therefore better suited to lower-intensity, longer duration exercise or activity.

As described above, the systems of glycolysis, oxidative phosphorylation, and high-energy phosphate transfer must become more active to adapt to higher ATP demand during exercise. However, these processes create byproducts that impair Na^+/K^+ balance, intracellular Ca^{2+} handling, and crossbridge cycling that may result in the fatigue of the highly activated muscle (Green, 1997). Most importantly, there is a failure in excitation-contraction coupling at the junction between t-tubules; this failure has been demonstrated to be long-lasting and may result in prolonged depression of contractile force production that lasts long after the initial fatiguing event (Bruton *et al.,* 1998). Fatigue is actually vital to preserving muscle function in the long-term, protecting against the depletion of ATP to levels low enough to cause rigor or even irreversible damage to muscle tissue (Baker *et al.,* 2010).

The free radical $NO^{\bullet}$ (nitric oxide; NO) functions as a versatile signaling molecule in numerous biological systems (Cheng *et al*., 2016). NO is synthesized enzymatically by nitric oxide synthase (NOS) in the presence of oxygen from L-arginine, or from the inorganic ions nitrate and nitrite (NO_3^- and NO_2^-,

respectively) when oxygen is limited (Cheng *et al*., 2016). NO production is upregulated during repeated contractions in skeletal muscle fibers (Cheng *et al*., 2016). NOS exists in many tissues, but specific NOS isoforms may be present in only some cell types. Furthermore, alternative splicing accounts for tissue-specific expression (Stamler & Meissner, 2001) of NOS isoforms. The known isoforms are neuronal NOS (nNOS), endothelial NOS (eNOS), and inducible NOS (iNOS). All three isoforms are present in skeletal muscle (Tengan *et al.*, 2012). nNOS and eNOS are constitutively expressed in skeletal muscle, while iNOS is upregulated in response to acute inflammation (Cheng *et al*., 2016). nNOS and eNOS are activated by high cytosolic Ca^{2+} concentrations by a Ca^{2+}-calmodulin-dependent mechanism (Piazza *et al*., 2012). The half-life of NO in skeletal muscle is ~0.3 seconds because although it is relatively stable, it reacts quickly with many intracellular targets (Cheng *et al*., 2016): NO is incorporated into organic molecules by downstream reactions known as S-glutathionylation, nitration, heme-NO, and S-nitrosylation (Tengan *et al.*, 2012).

Importantly, one downstream NO pathway reaction, S-nitrosylation, is responsible for the post-translational modification of intracellular proteins that may alter their function. GSNO, a molecule that carries NO and can act as an NO donor by transferring its NO group to other molecules, is produced by a reaction between NO and reduced glutathione (GSH). S-nitrosylation involves covalent attachment of an NO group to the thiol side chain of a cysteine (Hess *et al*., 2005). GSNO can then post-translationally modify intracellular proteins by transfer of the NO group to sulfhydryl (-SH) groups of cysteine residues within a particular protein; this type of reaction is called transnitrosylation (Hogg, 2002). Therefore, through transnitrosylation, GSNO functions as an NO reservoir and also enables NO to be delivered throughout the cell (Corpas *et al*., 2013). One product of the transnitrosylation reaction between a protein and GSNO is an S-nitrosylated protein, and concurrently GSNO is degraded into GSSG via oxidation (Corpas *et al*., 2013).

While NO is able to regulate intracellular targets via S-nitrosylation, its effects are counterbalanced by denitrosylation. S-nitrosoglutathione reductase (GSNOR) is an enzyme that has been shown to perform denitrosylation reactions (Moon *et al.*, 2017). GSNOR was first discovered for its role as an alcohol dehydrogenase (ADH) class III enzyme (Jensen *et al.*, 1998), but its presence in myofibers and its ability

to affect post-translational modification of proteins (Barnett & Buxton, 2017) makes the enzyme particularly interesting to study in relation to muscle fatigue. Previous research has identified GSNOR as a protective enzyme against excessive S-nitrosylation of intracellular proteins during fatiguing contractions (Foster *et al.*, 2003). This is because GSNOR degrades GSNO and upregulates formation of GSH, an antioxidant (Moon *et al.*, 2017). Therefore, GSNOR curbs protein S-nitrosylation by limiting GSNO availability (Foster *et al.*, 2003). Mouse hepatocytes that lacked GSNOR had higher levels of S-nitrosylated proteins after iNOS was induced, suggesting that GSNO is responsible for this type of protein modification (Foster *et al.*, 2003).

The regulation of S-nitrosylation has been shown to be important under both physiological and pathologic conditions. NO in muscle has been found to act partially through S-nitrosylation of cysteines (Stamler & Meissner, 2001). For example, S-nitrosylation of cysteine residue 3536 of RyR1 has been shown to increase open channel probability and cause greater Ca^{2+} release under physiological oxygen conditions (Moon *et al.*, 2017). However, under pathological conditions hypernitrosylation of RyR1 leads to Ca^{2+} leak, or increased open channel probability that is implicated in skeletal muscle damage and associated with diseases including Duchenne and Becker muscular dystrophy, sarcopenia, and rheumatoid arthritis (Stamler & Meissner, 2001; Moon *et al.*, 2017). Changes in the regulation of posttranslational modification of proteins by S-nitrosylation of cysteine residues, caused by dysregulation of GSNOR, results in downstream consequences including diseases such as asthma, cystic fibrosis, and interstitial lung disease, making it a great potential therapeutic target (Barnett & Buxton, 2017). GSNOR may therefore contribute significantly to regulation of health by modulating protein S-nitrosylation (Barnett & Buxton, 2017) and preventing pathological states caused by dysregulation of S-nitrosylation. A clear link, however, has not yet been found to establish GSNO as a major source of S-nitrosylated proteins in skeletal muscle particularly during muscle fatigue (Moon *et al.,* 2017). Therefore, understanding which proteins are targets of S-nitrosylation and how this type of modification affects fatigue tolerance and recovery is critical to revealing the role of GSNOR in exercising and pathologic skeletal muscle.

METHODS

Reagents:

FURA-2 (Pentapotassium Salt, cell impermeant solubilized in 150 mM NaCl and 10 mM HEPES, pH 7.0) – Invitrogen Cat No. F1200.

GSNOR$_i$ (SPL-334; 4-{[2-[(2-Cyanobenzyl)thio]-4-oxothieno[3,2-d]pyrimidin-3(4H)-yl]methyl}benzoic acid solubilized in 0.1 M DMSO) – Sigma Aldrich Cat No. SML1880.

L-NMMA (NG-Methyl-L-arginine acetate salt) – Cayman Chemicals Cat No. 10005031.

All other reagents were purchased from Sigma Aldrich.

Ethical Approval:

All experimental procedures perform in animals were approved by the University of California San Diego Institutional Animal Care and Use Committee (IACUC; protocol # S00250).

Animals:

12–16-week-old male C57BL/6J mice (total of 19 mice) obtained from The Jackson Laboratory (Bar Harbor, ME, USA) were used for all experimental procedures. Mice were fed a standard diet with *ad libitum* access to food and water. On the day of the experiment, the animals were euthanized by an overdose of sodium pentobarbital (Fatal Plus, 150 mg/kg body weight), administered by a single intraperitoneal injection followed by cervical dislocation. Immediately after death the flexor digitorum brevis (FDB) or extensor digitorum longus (EDL) muscles were harvested from both feet and hindlimbs, respectively.

Experimental setup for intact extensor digitorum longus (EDL) muscles:

EDLs were carefully dissected with tendons attached and placed in Tyrode's dissecting solution (in mM: 134 NaCl, 5 KCl, 1.8 $CaCl_2$, 0.5 $MgCl_2$, 0.4 NaH_2PO_4, 11 $NaHCO_3$, 5.5 Glucose, pH 7.4). The EDL muscles were mounted to chambers (800MS Danish Myo Technology) by silk sutures tied around tendons on each end of the muscle. Muscles in the chambers were perfused with Tyrode's solution (in mM: 121 NaCl, 5 KCl, 1.8 $CaCl_2$, 0.5 $MgCl_2$, 0.4 NaH_2PO_4, 24 $NaHCO_3$, 5.5 Glucose, 0.1 EGTA, pH 7.4) and

bubbled with 95% O_2 and 5% CO_2 at 22ºC (Figure M1). An analog-digital converter (MP100, BIOPAC Systems, Inc) was used to convert the analog signal to a digital one, and the force acquisition data were analyzed using AcqKnowledgeIII 3.2.6 software (BIOPAC Systems). After 10 min of perfusion, the length of the muscles was adjusted to achieve maximal isometric twitch force (L_0) evoked by single twitches (1 pulse per second (Hz), 0.5 ms pulses, 16 V) using an S88X stimulator (Grass Technologies).

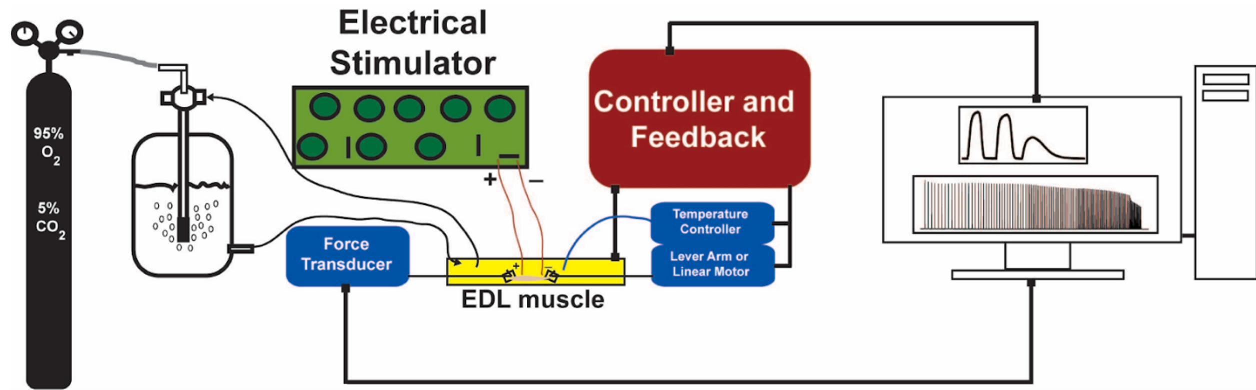

Illustration 2. Scheme of the intact EDL muscle system used in this study.

Experimental procedure to determine the effects of $GSNOR_i$ on EDL time to fatigue (EDL Protocol #1):

Muscles were allowed to rest for 10 min after finding L_0. Muscles were then subjected to a force-frequency (FF) Protocol (0.5 ms pulses, 16 V, 1-150 Hz, 300 ms trains once every 100 sec). After a 10 min rest following the FF Protocol, a fixed time period repetitive contraction protocol (EDL Fatigue Protocol #1) was performed, which consisted of repetitive contractions (100 Hz stimulations) at a rate of 0.33 trains per second (tps) for 2 min to fatigue the muscles. For each mouse, the muscles from both legs were stimulated simultaneously. Following the EDL Fatigue Protocol #1, the muscles were allowed to rest 1 hour; in the last 20 min of rest, $GSNOR_i$ (10 μM) was added to the perfusion solution of one EDL per mouse, while the contralateral EDL served as a non-treated control. Then, the EDL Fatigue Protocol #1 was repeated in the presence of $GSNOR_i$ or untreated for control muscles. After the contractility protocols, muscle length was measured, muscles were blotted dry and weighed, and cross-sectional area (CSA; in

mm^2) was determined by dividing muscle mass (in mg) by the product of muscle length (in mm) and muscle density (1.06 mg/mm^3) (Nogueira *et al.*, 2018). Force (kilopascal; kPa) was determined by normalizing absolute force developed (in millinewtons; mN) to the CSA (in mm^2) for each muscle.

Illustration 3. Scheme of EDL Protocol #1.

Experimental procedure to determine the effects of $GSNOR_i$ on EDL fatigue recovery (EDL Protocol #2):

In a separate group of mice, EDL muscles were allowed to rest for 10 min after finding L_0, and then subjected to the same FF protocol as in EDL Protocol #1: 0.5 ms pulses, 16 V, 1-150 Hz, 300 ms trains once every 100 sec. Then, $GSNOR_i$ (10 µM) was added to the perfusion solution of one EDL per mouse, while the contralateral EDL served as a non-treated control. In another set of muscles, $GSNOR_i$ and NOS inhibitor L-NMMA were added together to the perfusion solution. After 20 min of incubation with $GSNOR_i$, a second FF was performed in both muscles to test whether the addition of $GSNOR_i$ produced any shift in the FF response. After a 10 min rest following the second FF curve, EDL Fatigue Protocol #2 was performed, which consisted of repetitive contractions (100 Hz stimulations) at a rate starting at 0.25 tps for the first minute and then increasing the train rate by 1.2x each minute until the force developed fell to 30% of initial force output. For each mouse, the muscles from both legs were stimulated simultaneously. Force production for all muscles was measured 10-, 30-, 60-, and 120-min following fatigue. The muscles were stimulated at 30 Hz, 50 Hz, and 120 Hz during each time increment with 100 seconds between stimulations to track the recovery post-fatigue at submaximal (30 and 50 Hz) and maximal (120 Hz) frequencies of stimulation. After the experimental procedures with the muscles, muscle length was measured, muscles were blotted dry and weighed, and CSA was determined as described above.

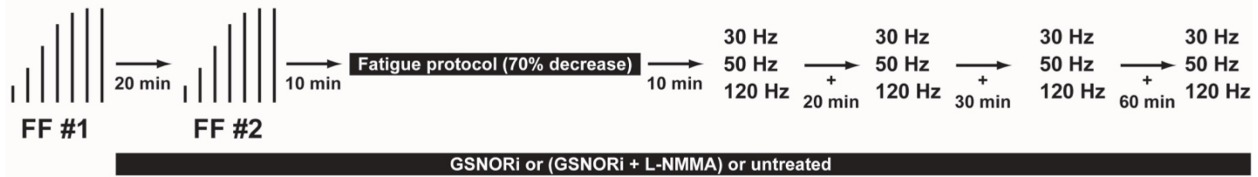

Illustration 4. Scheme of EDL Protocol #2.

Experimental setup for flexor digitorum brevis (FDB) Single Myofibers:

Intact single myofiber isolation from FDB muscle and FURA-2 loading:

FDB muscles from both feet were dissected and single muscle fibers with tendons intact were mechanically dissected under dark field illumination in a dissecting solution (~4ºC; 136 mM NaCl, 5 mM KCl, 1.8 mM $CaCl_2$, 0.5 mM $MgCl_2$, 0.4 mM NaH_2PO_4, 11.9 mM $NaHCO_3$ and 5.5 mM glucose). After dissection, each myofiber was pressure injected with FURA-2, a fluorescent probe that binds to intracellular Ca^{2+}. The myofiber was allowed to rest for 20 min following FURA-2 microinjection, and platinum clips were attached to the tendons on each end of the myofiber, and then mounted onto a Small Intact Muscle Apparatus (model 1500A, Aurora Scientific) to measure myofiber force development and intracellular fluorescence.

The analog signal was converted to digital one and analyzed as described for EDL muscle. The apparatus was placed on the stage of an inverted microscope for epifluorescence (Nikon Eclipse Ti-S with a 40x long distance Fluor objective and integrated with a Photon Technology International (Birmingham, NJ, USA) illumination and detection system (DeltaScan model)). The chamber housing the intact single myofiber was perfused with Tyrode's solution (in mM: 121 NaCl, 5 KCl, 1.8 $CaCl_2$, 0.5 $MgCl_2$, 0.4 NaH_2PO_4, 24 $NaHCO_3$, 5.5 Glucose, 0.1 EGTA, pH 7.4), and bubbled with 20% O_2 and 5% CO_2 at 22ºC.

Cytosolic Ca^{2+} ($[Ca^{2+}]_c$) measurements:

$[Ca^{2+}]_c$ was recorded simultaneously to contractility during each FF protocol. FURA-2 injected myofibers were illuminated with two rapidly alternating (200 Hz) excitation wavelengths of 340 and 380

nm. The ratio of fluorescence excitation (340 nm/380 nm; R) at an emission length of 510 nm was obtained. Fluorescence was converted to $[Ca^{2+}]_c$ according to the following equation (Nogueira *et al.,* 2018):

$$[Ca^{2+}]_c = K_D\beta[(R - R_{min})/(R_{max} - R)]$$

In the above equation, K_D is the dissociation constant for Ca^{2+}-FURA-2 and was set to 224 nM. β is the ratio of fluorescence between high and no $[Ca^{2+}]_c$ at 380 nm; β was determined for each contracting myofiber as described by Gandra *et al.,* (2018). R_{min} is the fluorescence ratio at low $[Ca^{2+}]_c$ when Ca^{2+}-FURA-2 binding is minimal (set to 0.24), and R_{max} is the fluorescence ratio found at high $[Ca^{2+}]_c$ when binding is maximal. R_{max} was set to 136% of the peak ratio obtained during contraction at maximal force (with 80-100 Hz stimulations) in the presence of 10 mM caffeine before fatigue or treatments (FF#1; details below). To obtain the peak $[Ca^{2+}]_c$ during contractions, the average FURA-2 fluorescence ratio in the final 100 ms of stimulation was used.

Experimental procedure to determine the effects of $GSNOR_i$ on FDB intact single myofiber post-fatigue force and intracellular Ca^{2+} handling:

Myofiber L_0 was determined using tetanic contractions (set with 80-100 Hz stimulations, 300 ms trains, 0.5 ms pulses, 8V, evoked with an S88X stimulator (Grass Technologies)), and allowed to rest for 10 min. The first FF (FF#1) measurements (1-150 Hz once every 100 sec) were collected to obtain a baseline for the force and Ca^{2+} measurements pre-fatigue. Immediately after the last frequency of stimulation, the myofiber was switched to a perfusion solution of Tyrode supplemented with 10 mM caffeine, followed by a tetanic stimulation at 80-100 Hz, then re-perfused with Tyrode perfusion solution without caffeine. 10 min after caffeine washout following FF#1, a fatigue protocol similar to the EDL Fatigue Protocol #2 (FDB Fatigue Protocol) was performed, which consisted of repetitive contractions at 80-100 Hz at a rate starting at 0.25 tps for the first minute and then increasing the train rate by 1.2x each minute until the myofiber retained 50% of its initial force. The myofiber was allowed to rest for 30 min after Fatigue #1, and then a second FF (FF#2) was performed to determine the persistent effects of fatigue on force and $[Ca^{2+}]_c$. After FF#2, the myofiber was incubated for 20 minutes with either $GSNOR_i$ (10 μM) or DMSO (vehicle), which were added to the perfusion solution. A third FF (FF#3) was performed,

followed by a Fatigue #2. The myofiber was allowed to recover for 30 min from Fatigue #2, and the final FF (FF#4) was performed to determine the effects of GSNOR$_i$ (or vehicle) on post-fatigue force and $[Ca^{2+}]_c$. Force development (in mN) was normalized to the CSA (in mm^2) determined from the diameter of the myofiber and data are reported as kPa.

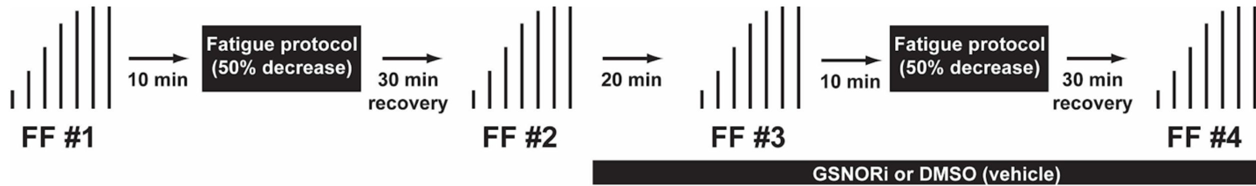

Illustration 5. Scheme of FDB single myofiber protocol.

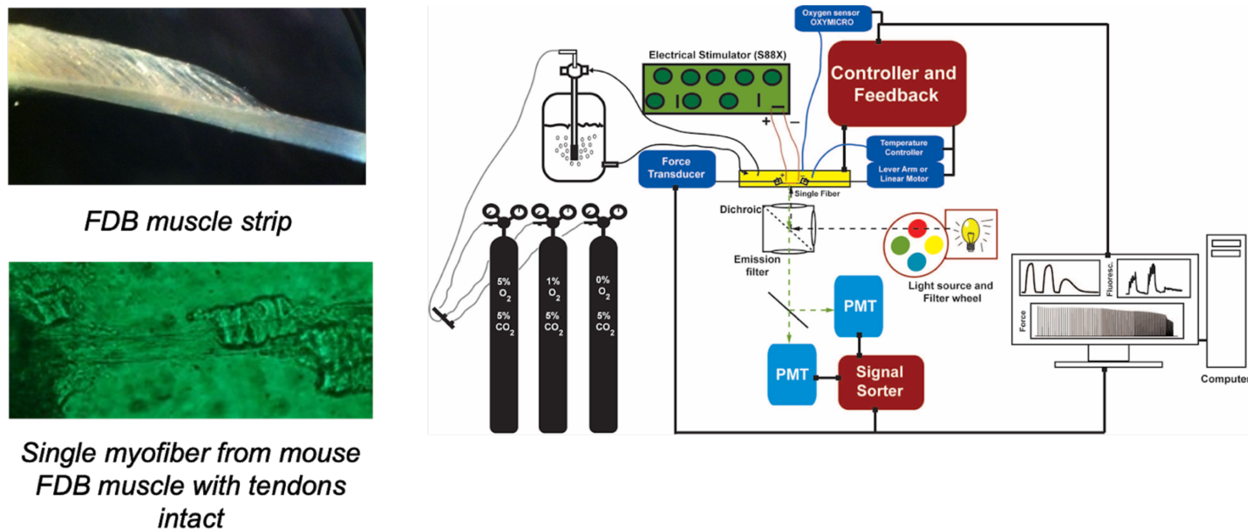

Illustration 6. Scheme of experimental setup for the FDB single myofiber protocol.

Statistical analyses:

The experimental results are presented as mean ± standard error (s.e.). For comparison between two groups, paired Student's *t*-test was used. For multiple comparisons, a one-way ANOVA followed by the Tukey post-test or a two-way ANOVA followed by a Bonferroni post-test was used using a Prism 4.0 software (GraphPad). $P<0.05$ was considered to represent a significant difference.

RESULTS

We investigated the role of GSNOR on NO-dependent effects in myofibrillar and Ca^{2+}-handling functions before, during and after fatigue in skeletal muscle.

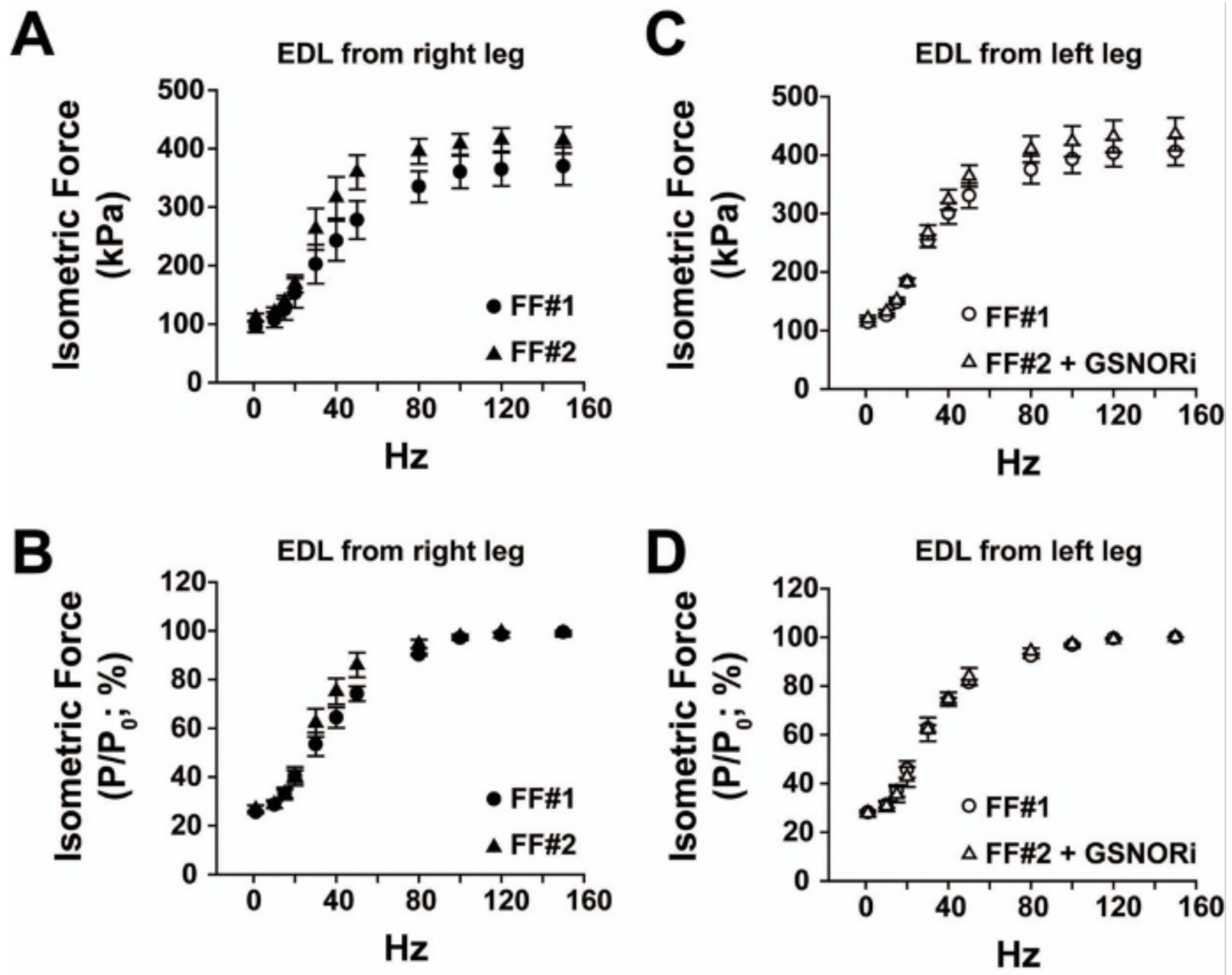

Figure 1. EDL Protocol #2: Force-frequency curves from EDL muscles before and after 20 min incubation with either GSNOR$_i$ (10 µM; FF#2) incubation or untreated.
A and C) Force developed by EDL muscles normalized by the cross-sectional area (kPa); B and C) Force normalized by the maximal tension (P/P_0). Mean ± SE (n = 6 mice). A) P<0.0001 vs FF#1 (Two-way ANOVA repeated measures), P<0.05 vs FF#1 (40 and 50 Hz, Bonferroni post-test). B) P<0.003 vs FF#1 (Two-way ANOVA repeated measures), P<0.05 vs FF#1 (40 and 50 Hz, Bonferroni post-test). C) P<0.0001 vs FF#1 (Two-way ANOVA repeated measures), P<0.05 vs FF#1 (80 and 150 Hz, Bonferroni post-test). D) P<0.0497 vs FF#1 (Two-way ANOVA repeated measures), P>0.05 vs FF#1 (Bonferroni post-test).

EDL Protocol #2 showed that the incubation of muscles for 20 min with either $GSNOR_i$ or untreated (control) did not affect contractile function under non-fatiguing conditions. FF curves were measured for EDL muscles treated with $GSNOR_i$ (left leg) versus their contralateral (right leg) muscles used as controls, from mice to measure the force production at a range of stimulation frequencies (Figure 1). Data from FF curves, which take on a sigmoidal trend, allow for comparisons of both submaximal and maximal force measurements between different muscles under non-fatiguing contractions, as the muscle is allowed to recover for 100 sec between each stimulation. The mean force generated by the control EDL muscles between FF#1 and FF#2 were not statistically different (Figure 1A, B). The mean force generated by EDL muscles treated with $GSNOR_i$ also showed no statistical difference in force production between FF#1 and FF#2 (Figure 1C, D). This indicates that $GSNOR_i$ does not alter force development of muscles under non-fatiguing conditions relative to untreated control muscles.

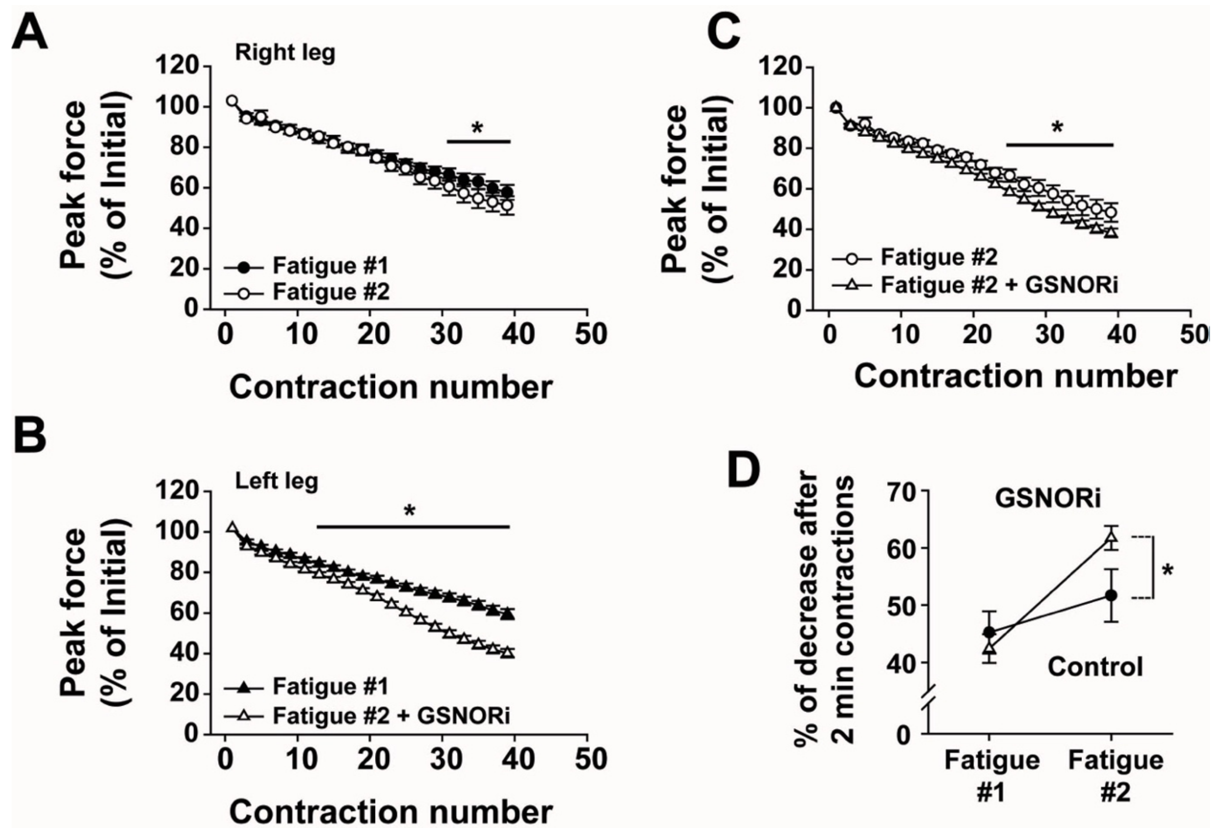

Figure 2. EDL Protocol #1: Force development during repetitive contractions evoked by 100 Hz stimulations each 3 seconds (0.33 tps) for 2 min.

Mean ± SE (n=6 mice). A) Time course of the decrease in force during repetitive contractions during a fixed interval fatigue protocol. A) $P<0.0001$ vs Fatigue #1 (Two-way ANOVA repeated measures), $P<0.05$ vs Fatigue #1 (contractions 31-39, Bonferroni post-test). B) $P<0.0001$ vs Fatigue #1 (Two-way ANOVA repeated measures), $P<0.05$ vs Fatigue #1 (contractions 13-39, Bonferroni post-test). C) $P<0.0001$ vs Control, $P<0.05$ vs control (contractions 25-39, Bonferroni post-test). D) $P<0.05$ vs control for Fatigue #2.

We were able to determine with EDL Protocol #1 that $GSNOR_i$ impaired the muscles' ability to produce force during fatiguing conditions; the $GSNOR_i$ treated EDL were fatigued to a higher degree than the control EDL in a fixed time period fatigue protocol (Figure 2). Force production during the time course of a fatigue bout in muscles treated with $GSNOR_i$ showed lower force development vs the untreated muscles, during the 2-min contraction bout (Figure 2A, B). The percentage of decay in force at the last contraction of each fatigue bout (Fatigue #1 and Fatigue #2) was significantly higher in muscles which $GSNOR_i$. Furthermore, force production was more highly reduced compared to peak force toward the end of the fatigue run in $GSNOR_i$ treated muscles (Figure 2C), with $GSNOR_i$ treated muscles showing a

statistically significant higher decrease in force at the end of the fatigue bout (Figure 2D). While the force toward the end of Fatigue #2 was statistically higher than Fatigue #1 in the control group, it is likely that the muscles recovered a small amount of force due to spending longer time in the perfusion chamber. These data indicate that GSNOR indeed has a protective effect on contractile force during fatigue.

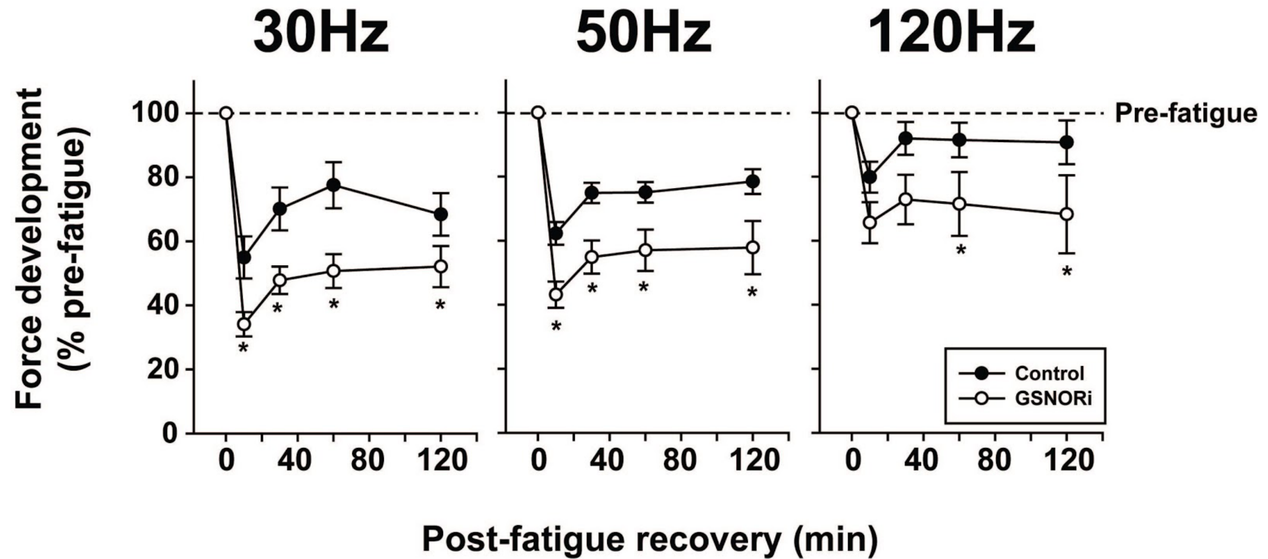

Figure 3. EDL Protocol #2: Time course of force recovery after a fatigue protocol at submaximal (30 and 50 Hz) and maximal (120 Hz) frequencies of stimulation.
Mean ± SE (n=6 mice). *P<0.05 vs control (Bonferroni post-test).

EDL Protocol #2 allowed us to track the recovery of force following fatigue in EDL muscles treated with $GSNOR_i$ compared to untreated controls, since muscles were fatigued until force had fallen to 30% of the initial. Tracking the recovery of the control and $GSNOR_i$ treated muscles for 2 hr after a fatigue bout (Figure 3) demonstrates that at both submaximal (30 and 50 Hz) frequencies and maximal (120 Hz) frequencies of stimulation, the $GSNOR_i$ treated muscles produced significantly less force than the untreated controls. These data show that $GSNOR_i$ incubation inhibits recovery of contractile force in EDL muscles after a bout of fatigue.

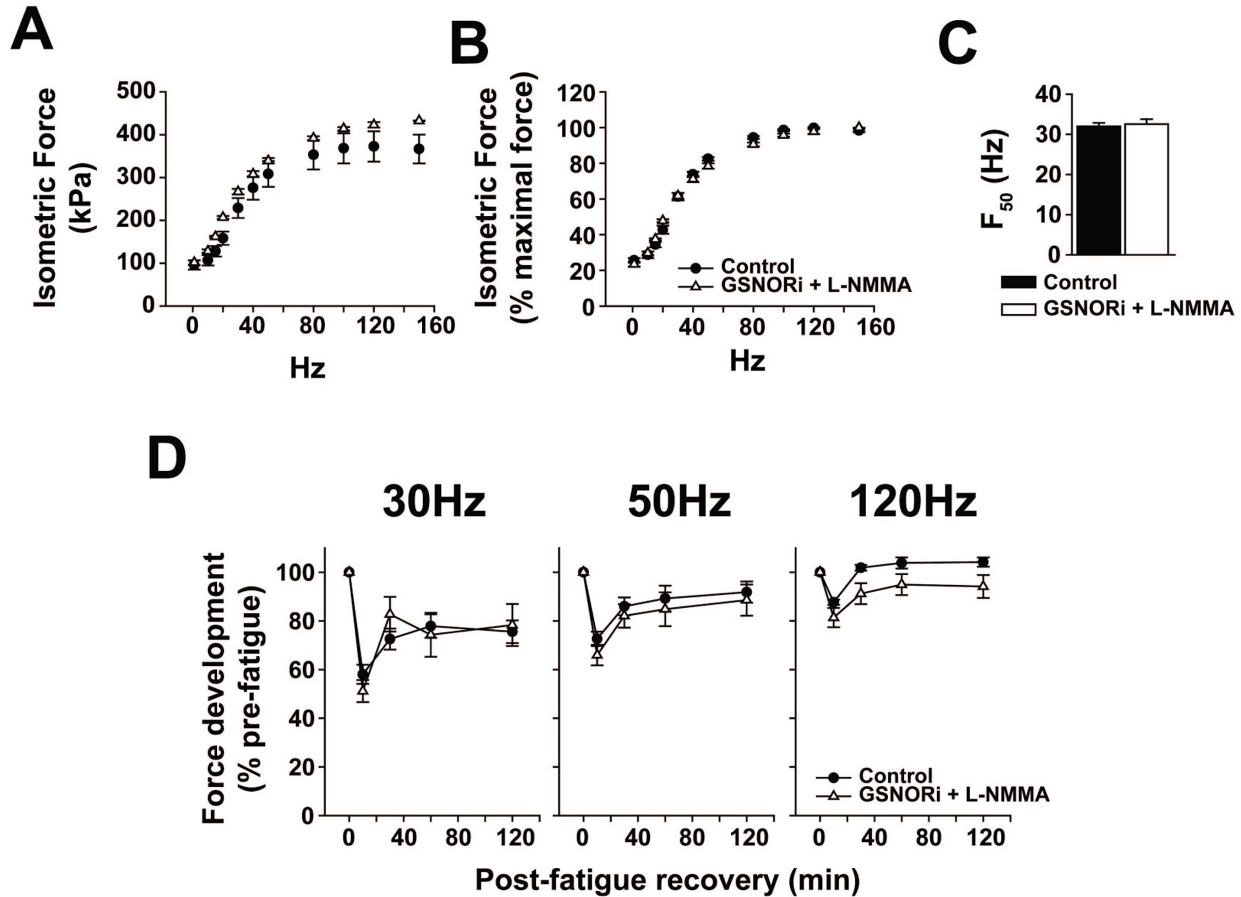

Figure 4. Effects of $GSNOR_i$ + L-NMMA incubation before and after EDL Protocol #2.
Isometric force in a FF protocol expressed in kPa (A) and as a percent of maximal force (B) show no statistical differences. The F_{50} (C) was also unchanged between groups. D) shows the time course of force recovery at submaximal (30 and 50 Hz) and maximal (120 Hz) frequencies of stimulation after a fatigue protocol was performed. Mean ± SE (n=5). P>0.05 vs control for 30 Hz and 50 Hz recoveries (Bonferroni post-test), P=0.0004 vs control at 120 Hz recovery (Two-way ANOVA).

To test whether the effects seen with $GSNOR_i$ on EDL muscles were dependent on NO production during contractions, the NOS inhibitor L-NMMA was incubated together with $GSNOR_i$, so GSNO would not be formed by contraction-induced NO production. The results of Figure 4 indicate that adding L-NMMA together with $GSNOR_i$ prevented the depressed force recovery after a fatigue bout that we observed in Figure 3 with $GSNOR_i$ alone. The FF curves, as well as the F_{50} (the midpoint of the FF curve), were not statistically different (Figure 4A-C). There was a statistically significant difference in the post-fatigue recovery period between untreated muscles and muscles treated with $GSNOR_i$ and L-NMMA, but only for 120 Hz, whereas the difference was seen at all stimulation frequencies (30, 50, and 120 Hz) for the control

vs. the $GSNOR_i$ group. This indicates that contraction-induced NO production leads to an increase in GSNO that would be reduced by GSNOR, preventing GSNO-dependent effects in post-fatigue contractility.

We used an ex-vivo FDB single myofiber model to try to further elucidate the effects of GSNOR inhibition. Our goal was to determine whether the myofibrillar and/or Ca^{2+} handling sites were altered by measuring force in tandem with cytoplasmic Ca^{2+} transients. We did this for each myofiber during FF protocols before and after fatigue with addition of $GSNOR_i$ (FDB single myofiber protocol).

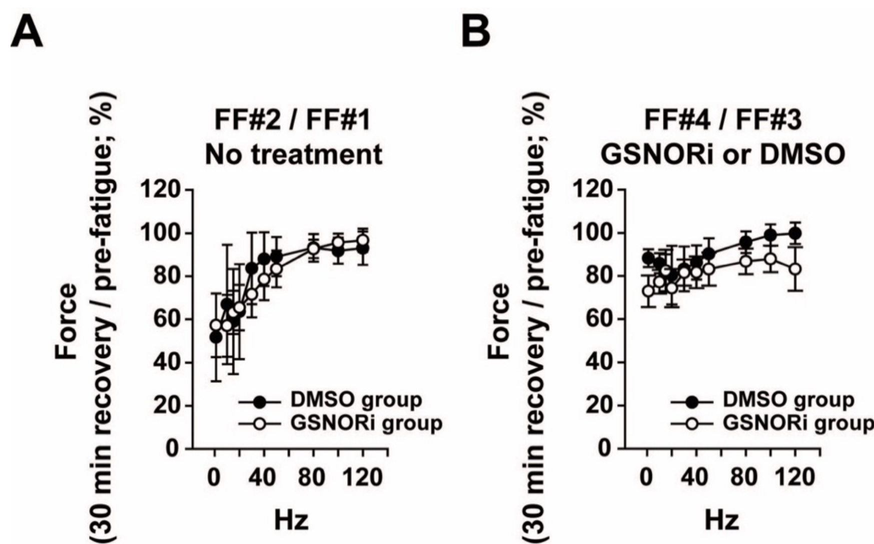

Figure 5. Percentage of force evoked by each frequency of stimulation 30 min after Fatigue #1 (A) and Fatigue #2 (B) compared to pre-fatigue force development in the single myofiber protocol. Myofibers were treated with either $GSNOR_i$ or DMSO before Fatigue #2. Mean ± SE, n = 4 for DMSO group and n=5 for $GSNOR_i$ group. A) $P>0.05$ vs DMSO group (Two-way ANOVA); B) $P=0.0263$ ($P<0.05$) vs DMSO group (Two-way ANOVA).

We first compared the force produced during each FF before and 30 min after fatigue of the single myofibers (Figure 5). We compared both the $GSNOR_i$ and DMSO groups to their pre-fatigue force expressed as a percentage before treatment (Figure 5A): force produced in FF#2 compared to FF#1 (Fatigue #1); and after GSNOR or DMSO treatment: force produced in FF#4 compared to FF#3 (Fatigue #2; Figure 5B). There was a prolonged low frequency force depression (PLFFD) effect in both groups, which can be expected after a bout of fatiguing contractions (Chaillou & Cheng, 2019). However, we also determined

that the fibers treated with $GSNOR_i$ exhibited a statistically significant lower force recovery (after 30 min of recovery from Fatigue #2) than the DMSO group in FF#4 compared to FF#3. This finding is similar to that of the EDL contractility data, showing that single myofibers, as well as intact muscle, exhibit a depressed force recovery after fatigue with GSNOR inhibition.

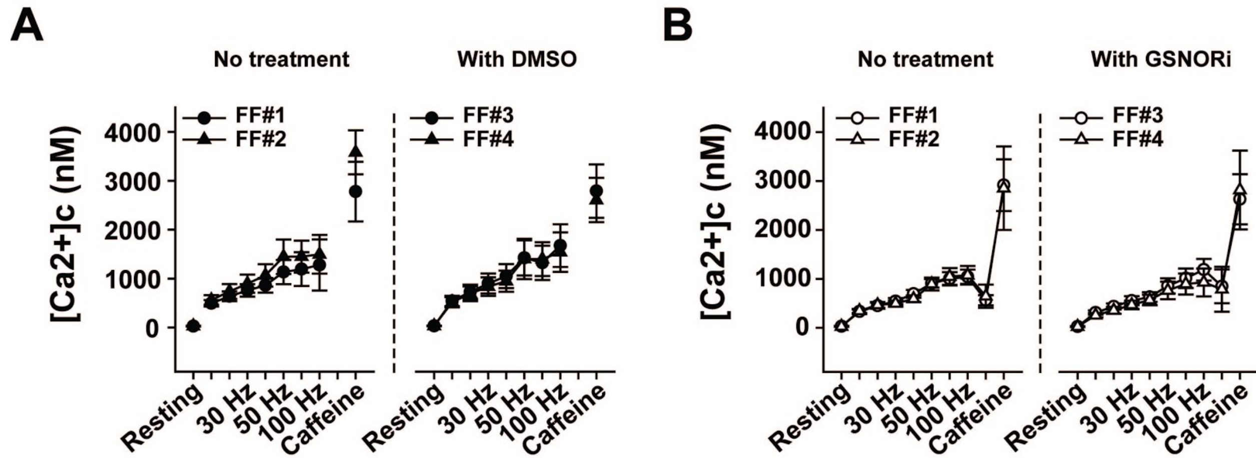

Figure 6. Cytosolic Ca^{2+} concentration ($[Ca^{2+}]_c$) measured during FF protocols before and 30 min after a fatigue bout before treatments (A) and after treatment with either 10 µM $GSNOR_i$ (n=5) or DMSO (vehicle) in FDB myofibers (n=4) (B).
Mean ± SE. P>0.05 vs FF#1 or FF#3, two-way ANOVA.

The cytosolic Ca^{2+} transients of single myofibers measured during each stimulation of each FF protocol allowed us to compare the $[Ca^{2+}]_c$ before and after fatigue treatment, with or without $GSNOR_i$ (Figure 6). There was no statistical difference in Ca^{2+} transients between FF#1 and FF#2 or FF#3 and FF#4 between the groups of myofibers, independent of DMSO (Figure 6A) and $GSNOR_i$ (Figure 6B) treatments. We thus were unable to observe any $GSNOR_i$-mediated effect on $[Ca^{2+}]_c$ in these experiments.

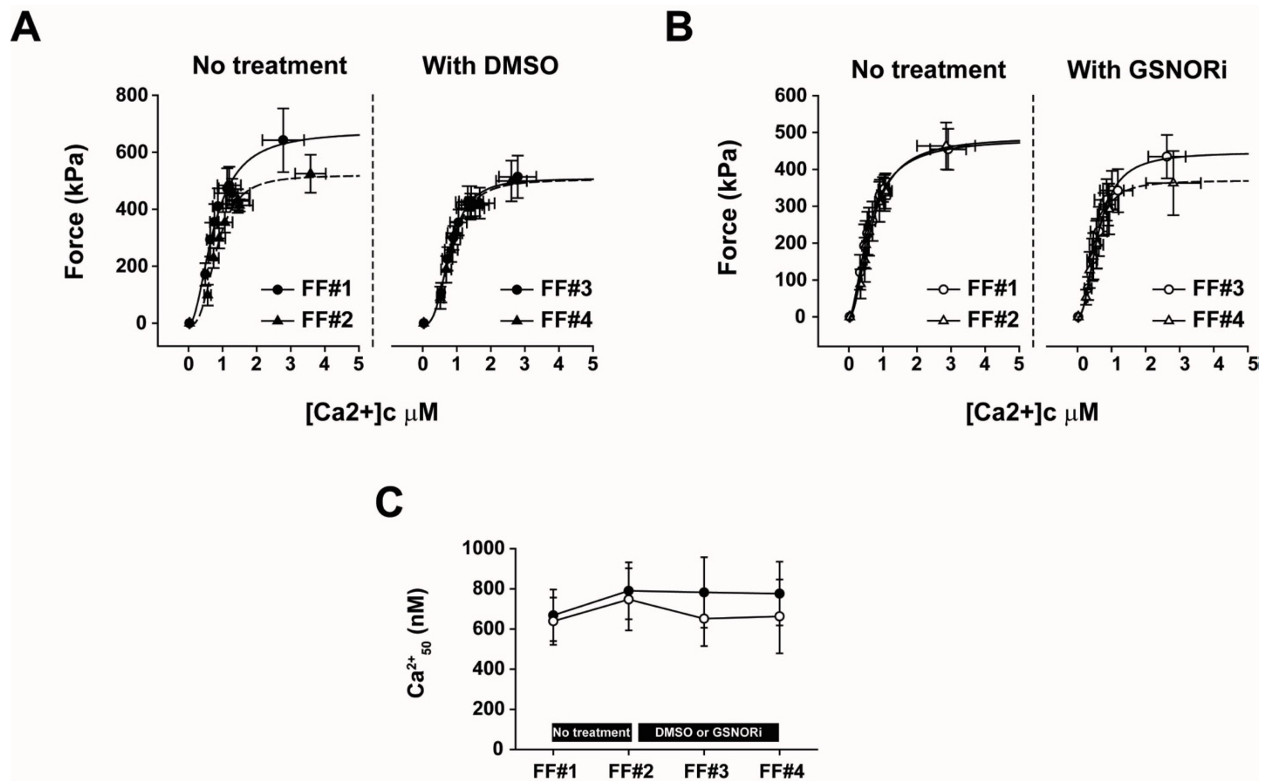

Figure 7. Mean data showing the $[Ca^{2+}]_c$-Force relationship for DMSO (n=4) (A) and $GSNOR_i$ (n=5) (B) treated myofibers.
The figure compares the $[Ca^{2+}]_c$-Force relationship before and after each of the fatigue protocols, which occurred between FF#1 and FF#2, and between FF#3 and FF#4. In C) we compare the midpoint of the $[Ca^{2+}]_c$-force relationship determined by a sigmoid equation (Ca^{2+}_{50}) for $GSNOR_i$ (n=5) and DMSO (n=4) treated fibers during each FF curve. Mean ± SE. ($P>0.05$ vs DMSO treatment, two-way ANOVA).

We then sought to determine whether there was a change in the force-Ca relationship to detect any changes in Ca^{2+} sensitivity (Figure 7). We found there was no statistical difference in the $[Ca^{2+}]_c$-Force relationship 30 min after fatigue for either DMSO or $GSNOR_i$ groups (Figure 7A, B). Figure 7C demonstrates that there was no difference in the midpoint of the $[Ca^{2+}]_c$-force curve between $GSNOR_i$ and DMSO treated fibers during each of the FF protocols, suggesting that $GSNOR_i$ does not affect myofilament Ca^{2+} sensitivity.

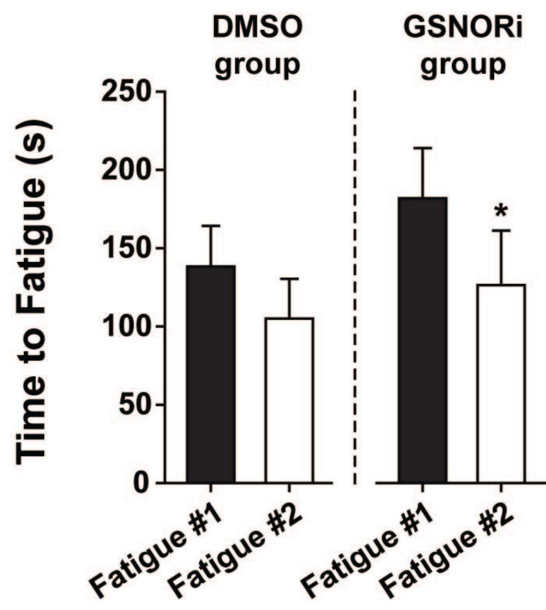

Figure 8. Mean time to fatigue for myofibers in Fatigue #1 (no treatment) vs. Fatigue #2 ((GSNOR$_i$) (n=5) or DMSO treatment (n=4)).
Mean ± SE. *$P<0.05$ vs Fatigue #1, paired t-test.

Our data indicate that there is no meaningful difference in time to fatigue between fibers treated with GSNOR$_i$ and fibers treated with DMSO (Figure 8). While we did find a statistical difference in the time to fatigue in Fatigue #2 compared to Fatigue #1 between GSNOR$_i$ and DMSO treated fibers, the DMSO group included one fiber that had a higher time to fatigue in the second fatigue compared to the first fatigue, which may account for the statistical differences in time to fatigue between groups. All of the other fibers in both experimental groups exhibited a decrease in the time to fatigue for the second fatigue compared to the first. There is not sufficient evidence in these experiments to be convinced that time to fatigue is affected by GSNOR$_i$.

DISCUSSION

There are many established experimental models to study fatigue in skeletal muscle, each of which comes with a unique set of benefits and limitations as outlined in the comprehensive review on muscle fatigue by Allen *et al.* (2008). Our research incorporates two of these methods — the isolated muscle model using mouse EDL muscles, and the isolated single fiber model using mouse FDB fibers — to elucidate the role of GSNOR in fatigue and during recovery post fatigue. The greatest advantage of the isolated muscle model is the ability to eliminate central fatigue since the muscle is dissected from the body and electrically stimulated directly instead of through the nerves. In addition, isolated muscles have the same proportion of myofiber types between mice of the same age and weight. However, this model is limited due to factors including: 1) not being able to isolate specific fiber types; 2) the accumulation of extracellular metabolic products between myofibers and in the perfusion media; and 3) slow perfusion of drugs to all fibers in the muscle. Advantages of the second model we used, the isolated single fiber model, include the ability to isolate specific fiber types, directly correlate force to other intracellular changes within the fiber, obtain fluorescence measurements of intracellular transients, and rapidly perfuse drugs or chemicals directly to the fiber. However, this method is not often used because of the difficulty to perform. It also has other disadvantages, including the experimental environment not being exactly same as in vivo, accompanied by the lack of changes observed in vivo such as K^+ accumulation.

An advantage of the whole isolated muscle experiments is that with each muscle there is a similar proportion of fiber types between mice, so the muscles can be easily compared. EDL are primarily composed of fast twitch (type II) fibers. A previous study which fiber-typed various C57BL6J mouse muscles found that their EDL are composed of 66.01 ± 8.51% IIB and 21.48 ± 7.33% IIDB fibers, with smaller proportions of IIAD, IC/IIC, IIA, and I fibers also observed (Augusto *et al.,* 2004). When performing experiments in single fibers from FDB muscles, it is not possible to differentiate between fast twitch myofibers before the experiment is performed. Instead, for the single fiber data we discarded highly oxidative fibers which had higher times to fatigue (>300 sec to lose 50% of force in the FDB Fatigue Protocol) in order to compile data on only the more fast-twitch fibers so we could compare the results to

those of the whole EDL muscles. By gathering data from both of these methods, we were able to get a better understanding of how GSNOR affects fatigue resistance on the whole muscle scale using isolated EDL muscles, as well as what occurs in the single fiber by recording force along with intracellular Ca^{2+} during and after fatiguing contractions. By analyzing the data together, we were able to correlate the findings to delineate the specific role of GSNOR in skeletal muscle fatigue resistance and post fatigue force recovery.

The results of these experiments demonstrate that the addition of $GSNOR_i$ did not affect production of contractile force under non-fatiguing conditions in both whole EDL muscles and FDB myofibers. These data also showed that whole EDL muscles treated with $GSNOR_i$ fatigued more quickly than untreated controls, but there was no such effect on fatigue observed in the single myofibers. However, both EDL muscles and FDB single myofibers exhibited prolonged depression of contractile force following a fatigue bout. These findings provide further evidence that GSNOR inhibition depresses fatigue resistance in skeletal muscle by allowing buildup of S-nitrosylated proteins through GSNO production.

The results from experiments following Protocol #2 comparing the FF curves of the mouse EDL muscles demonstrate that contractile function was not affected under non-fatiguing conditions when the muscles were incubated with $GSNOR_i$. The data from Figure 1 thus indicate that GSNOR does not play a large role in force development under non-fatiguing conditions. NO production is upregulated with repetitive contraction of skeletal muscle (Cheng *et al*., 2016); therefore, NO overproduction and, in turn, S-nitrosothiol buildup are not expected to occur under non-fatiguing conditions. Thus, because NO is not upregulated at rest, we would not expect to observe any differences in force between $GSNOR_i$ and control groups prior to a fatigue bout. The preservation of non-fatiguing contractile force in $GSNOR_i$ treated fibers also indicates it is unlikely that the chemical inhibitor is inherently toxic to the muscle tissue, but rather that the reduction in force observed in response to fatiguing the muscle is actually caused by enzymatic inhibition of GSNOR.

We were also able to determine that $GSNOR_i$ impaired the EDL muscles' ability to produce force during fatiguing conditions and during the recovery period following fatigue. The EDL treated with $GSNOR_i$ in Protocol #1 exhibited a significantly higher reduction in force relative to the peak force than

did the untreated controls (Figure 2), thereby indicating that GSNOR indeed has a protective effect during fatigue. This is consistent with our hypothesis that GSNOR is able to stop GSNO from S-nitrosylating myofibrillar and/or Ca^{2+}-handling sites and thus protect against changes in force production induced by GSNO. Furthermore, tracking the recovery post fatigue in EDL muscles treated with $GSNOR_i$ compared to untreated controls in Protocol #2, we showed that the $GSNOR_i$ treated muscles did not have a force recovery the same degree as the control muscles in the two hours following fatigue (Figure 3). This demonstrates that the muscles' ability to recover force was reduced for a prolonged period of time following fatigue when GSNOR was inhibited. Previous research has shown the modulatory effects of GSNO on the cysteine residues of contractile apparatus proteins via an S-nitrosylation mechanism (Andrade *et al.,* 1998; Nogueira, *et al.,* 2009; Dutka *et al.,* 2011; Dutka *et al.,* 2017), detailed later. These studies suggest, and our data supports, that in skeletal muscle, the S-nitrosylation of potentially numerous proteins may contribute to the reduced force production we observed in muscle fatigue. Our data showing that $GSNOR_i$ impairs force production during and after fatigue fits our hypothesized model that without GSNOR available to degrade GSNO, the dysregulation of protein S-nitrosylation causes excessive fatigue and a lowered capacity to recover from fatigue.

Another way we verified the specificity of $GSNOR_i$ was by perfusing the muscle with NOS chemical inhibitor L-NMMA simultaneously with $GSNOR_i$. It has been shown that L-NMMA is a nonselective inhibitor of NOS (Griffith & Kilbourn, 1996). The results from our L-NMMA experiments, shown in Figure 4, indicate that inhibiting NO production by blocking NOS activity attenuates the effects of $GSNOR_i$. Our data thus suggests that GSNOR is protective against the effects of GSNO, which is possibly produced during repetitive contractions. Therefore, according to our hypothesis the lower NO production due to L-NMMA perfusion would prevent excess GSNO accumulation and normal fatigue would be preserved. In our experiments, muscles treated with L-NMMA and $GSNOR_i$ do not exhibit the worsened fatigue resistance of $GSNOR_i$ treated muscles (Figure 4), supporting our hypothesis.

The single myofiber experiments allowed us to gain greater insights into the specific mechanisms by which GSNOR was affecting skeletal muscle in response to fatigue by measuring free intracellular

$[Ca^{2+}]$, which is important because its release is directly tied to force production (Mukund & Subramaniam, 2020). The single fiber method also allowed for a higher level of specificity in that any effect of $GSNOR_i$ on Ca^{2+} would be directly traceable to the force production of the single myofiber, which is not possible in the whole muscle experiments we performed in EDL.

With the microinjection of each myofiber with FURA-2 to measure intracellular free $[Ca^{2+}]_c$ (Nogueira *et al.,* 2018), we were able to determine whether myofilament Ca^{2+} sensitivity (Ca^{2+}-dependent force development) was affected by the presence of $GSNOR_i$. A study that treated mouse skeletal muscle fibers with pharmacological NO donors has shown NO to decrease myofibrillar Ca^{2+} sensitivity by inhibiting Ca^{2+} activation of actin filaments (Andrade *et al.,* 1998). Another group later used rat skinned skeletal myofibers treated with the NO donor S-nitroso-N-acetylpenicillamine (SNAP) and concluded that the Ca^{2+} sensitivity of the contractile apparatus was impacted, causing changes in submaximal force production (Dutka *et al.,* 2011). In a later study using exogenous GSNO and SNAP on skinned EDL and soleus myofibers from rats and skinned vastus lateralis muscles from humans, the authors detected S-nitrosylation of Cys134 on troponin I, leading to impaired myofibrillar Ca^{2+} sensitivity (Dutka *et al.,* 2017). By measuring $[Ca^{2+}]_c$ during each FF, we were able to compare Ca^{2+} handling under non-fatiguing conditions and 30 min post fatigue (Gandra *et al.,* 2018) for fibers in the absence and presence of $GSNOR_i$. Our data, as shown in Figure 6, indicates that since there were no statistical differences between the $[Ca^{2+}]_c$ measured during FF#4 of $GSNOR_i$ and DMSO group fibers following Fatigue #2, peak Ca^{2+} transients were not meaningfully altered by the buildup of S-nitrosothiols 30 min following fatigue. Furthermore, $GSNOR_i$ did not cause any changes in the force-Ca^{2+} relationship before and after fatigue (Figure 7), also suggesting that myofilament Ca^{2+} sensitivity was not impacted by $GSNOR_i$. Thus, according to our findings from Figures 6 and 7, the protective function of GSNOR must not be directly related to the protection of Ca^{2+}-handling sites, which seem to be unaffected by S-nitrosothiol buildup. Our results contradict data published previously (Andrade *et al.,* 1998; Dutka *et al.,* 2011; Dutka *et al.,* 2017) because while they found differences in myofiber Ca^{2+} sensitivity, we found no differences. The differences observed are likely due to differences in methodology. Whereas we used the intact single myofiber model and stimulated NO

production physiologically by fatiguing the myofibers, Andrade and colleagues treated single myofibers with excessive concentrations (much higher than physiologically expected) of NO donors, and Dutka and colleagues used a different technique (skinned fibers) and also used a pharmacological NO donor.

We determined from our single fiber experiments that the $GSNOR_i$ treated myofibers exhibited reduced recovery of maximal force production post fatigue (Figure 5), matching our findings from the EDL Protocol #2 experiments. This validates that the effects on fatigue we saw in the whole muscle experiments held up in a different experimental system. Prior research has demonstrated that NO modulates force production in skeletal muscle: rat diaphragm treated with an NO donor caused a reduction in submaximal force production, but the mechanism of action has not been elucidated (Heunks *et al.,* 1985). Prior publications have used NO donors to study the effects of NO on skeletal muscle contractility and Ca^{2+} handling (Andrade *et al.,* 1998; Dutka *et al.,* 2011; Dutka *et al.,* 2017; Heunks *et al.,* 1985), but our research takes a more physiological approach by stimulating NO production by the myofiber itself with fatiguing contractions instead of using a chemical NO donor. Myosin has previously been shown to be S-nitrosylated at numerous cysteine thiol sites; further, it was indicated that these modifications occur under transnitrosylation reactions with low-mass S-nitrosothiols (e.g., GSNO) instead of directly reacting with NO (Nogueira, *et al.,* 2009). Since force was impaired after fatigue with $GSNOR_i$ present, but no change in Ca^{2+} handling was detected, the effects of $GSNOR_i$ were likely due to modification of contractile sites. While we observed impaired force recovery post fatigue in $GSNOR_i$ treated fibers, we did not find a statistically significant change in the time to fatigue in the single fibers with $GSNOR_i$ treatment (Figure 8). The time to fatigue data from these FDB intact single fiber experiments differs from that of our EDL whole muscle data, in which we saw a faster time to fatigue for the muscles treated with $GSNOR_i$. It is unclear why we observed a decreased time to fatigue in the EDL but not the FDB experiments, but the changes in fatigue in the EDL may have been due to higher accumulation of metabolic byproducts, whereas no such accumulation would have occurred in the single fibers thus preserving force production for longer.

To reiterate, the worsened fatigue tolerance in EDL and prolonged depression of contractile force after fatigue of the EDL muscles and FDB single myofibers observed in this study is consistent with our

original hypothesis that GSNOR has a protective effect against the excessive S-nitrosylation of proteins involved in producing muscle contraction. These data support this hypothesis because the $GSNOR_i$, which blocks the action of GSNOR, prevents this enzyme from breaking down GSNO produced during contractions. Our data from the single myofiber experiments specifically suggest that the excess NO produced during muscle fatigue may lead to an increase in intracellular S-nitrosothiols by transfer from GSNO that impairs myofibrillar rather than Ca^{2+}-handling function.

These results fit into prior research which has described the protective effect of GSNOR in other tissues against the excessive S-nitrosylation of proteins by degrading GSNO. Evidence for this function was found by the observation that mouse hepatocytes which lacked GSNOR resulted in higher protein S-nitrosothiol levels after the induction of iNOS to produce NO (Foster *et al.,* 2003). It also expands on the 2017 paper by Moon and colleagues that found fatigue resistance was improved in $GSNOR^{-/-}$ mice. This group found that $GSNOR^{-/-}$ TA muscles exhibited excessive RyR1 S-nitrosylation which actually indicates that GSNOR negatively regulates force production, perhaps guarding against an imbalance in nitrosylation/denitrosylation that could cause muscle dysfunction. They also found that $GSNOR^{-/-}$ TA had reduced IIA fiber content but preserved mitochondrial content and function (Moon *et al.,* 2017). Although our data supports the proposed hypothesis that GSNOR has a protective effect against excessive S-nitrosylation of contractile proteins by GSNO buildup during fatigue, we cannot determine through these experiments alone which contractile proteins specifically are S-nitrosylated during fatigue.

Our data has provided more evidence that GSNOR shows a protective effect in skeletal muscle contractile force during and after fatigue, but future experiments should be done to further investigate the specific mechanism of this protective action. In order to directly show that GSNOR protects muscles from excessive S-nitrosylation, the biotin switch assay (Forrester *et al.,* 2009a) could be implemented to detect levels of S-nitrosylation on a tissue-wide scale in $GSNOR_i$ treated muscle tissue compared to control muscle tissue snap-frozen immediately after a fatigue bout. It would also be pertinent to unveil which specific myofibrillar proteins are S-nitrosylated by GSNO during physiologic fatiguing conditions. Another assay, S-nitrosothiol-resin assisted capture (SNO-RAC), with high specificity for high molecular weight proteins,

could be used to detect differences in S-nitrosylation of individual proteins (Forrester *et al.,* 2009b). Antibodies specific to proteins of interest (e.g., SERCA-1, ryanodine receptor-1 (RyR-1), myosin heavy chain (MHC)) can be implemented to measure differences in S-nitrosothiol levels for specific proteins isolated by SNO-RAC. This assay has high specificity, allowing for specific protein targets to be identified.

In conclusion, our results demonstrate that both whole EDL muscles and single FDB myofibers from mice exhibited reduced recovery from fatigue. Our data supports a mechanism in which the excess NO produced during muscle fatigue leads to an increase in intracellular S-nitrosothiols by transfer from GSNO that impairs contractile sites rather than Ca^{2+}-handling function. More work is required to determine which myofibrillar proteins are modified through this mechanism. These findings underlie a potential target for therapies to treat conditions in which GSNOR is dysregulated.

Material from this thesis is being prepared for submission for publication. The thesis author was the author of the material. Leonardo Nogueira and Michael C. Hogan were co-authors of the material.

REFERENCES

1. Allen, D.G., Lamb, G.D., Westerblad, H. (2008). Skeletal Muscle Fatigue: Cellular Mechanisms. *Physiol. Rev.* 2008(88):286-332. doi: 10.1152/physrev.00015.2007

2. Andrade, F.H., Reid, M.B., Allen, D.G., Westerblad, H. (1998). Effect of nitric oxide on single skeletal muscle fibres from the mouse. *J Physiol*. 509(Pt 2): 577-86. doi: 10.1111/j.1469-7793.1998.577bn.x

3. Augusto, V., Padovani, C.R., Eduardo, G., Campos, R. (2004). Skeletal muscle fiber types in c57BL6J mice. *Braz. J. morphol. Sci.* 21(2): 89-94.

4. Baker, J.S., McCormick, M.C., Robergs, R.A. (2010). Interaction among Skeletal Muscle Metabolic Energy Systems during Intense Exercise. *J. Nutr. Metab.* 2010: 905612. doi: 10.1155/2010/905612

5. Barnett, S.D., Buxton, I.L.O. (2017). The Role of S-nitrosoglutathione Reductase (GSNOR) in Human Disease and Therapy. *Crit. Rev. Biochem. Mol. Biol.* 52(3): 340–354. doi:10.1080/10409238.2017.1304353

6. Bruton, J.D., Lännergren, J., Westerblad, H. (1998). Mechanisms underlying the slow recovery of force after fatigue: importance of intracellular calcium. *Acta Physiol. Scand*. 162: 285-293. 10.1046/j.1365-201X.1998.0292f.x

7. Chaillou, T., Cheng, A.J. (2019). Mechanisms of prolonged low-frequency force depression: in vivo studies get us closer to the truth. *Am. J. Physiol. Regul. Integr. Comp. Physiol.* 316(5), R502-R503. doi: 10.1152/ajpregu.00063.2019

8. Cheng, A.J., Yamada, T., Rassier, D.E., Anderson, D.C., Westerblad, H. (2016). Reactive oxygen/nitrogen species and contractile function in skeletal muscle during fatigue and recovery. *J. Physiol.* 594(18): 5149-5160. doi: 10.1113/JP270650

9. Cooke, R. (2004). The Sliding Filament Model. *J. Gen. Physiol.* 123(6): 643-656. doi: 10.1085/jgp.200409089

10. Corpas, F.J., Alche, J.D., Barroso, J.B. (2013). Current overview of S-nitrosoglutathione (GSNO) in higher plants. *Front. Plant Sci.* Vol. 4. doi: 10.3389/fpls.2020.00651

11. D'Souza, D.M., Al-Sajee, D., Hawke, T.J. (2013). Diabetic myopathy: impact of diabetes mellitus on skeletal muscle progenitor cells. *Front. Physiol.* 2013(4): 379. doi: 10.3389/fphys.2013.00379.

12. Dutka, T.L., Mollica, J.P., Posterino, G.S., Lamb, G.D. (2011). Modulation of contractile apparatus Ca^{2+} sensitivity and disruption of excitation-contraction coupling by S-nitrosoglutathione in rat muscle fibres. *J. Physiol*. 589(Pt 9): 2181-2196. doi:10.1113/jphysiol.2010.200451

13. Dutka, T.L., Mollica, J.P., Lamboley, C.R., Weerakkody, V.C., Greening, D.W., Posterino, G.S., Murphy, R.M., & Lamb, G.D. (2017). *S*-nitrosylation and *S*-glutathionylation of Cys134 on

troponin I have opposing competitive actions on Ca^{2+} sensitivity in rat fast-twitch muscle fibers. *Am. J. Physiol. Cell. Physiol*. 312(3): C316-C327. doi: 10.1152/ajpcell.00334.2016

14. Forrester, M.T., Foster, M.W., Benhar, M., Stamler, J.S. (2009a). Detection of protein S-nitrosylation with the biotin-switch technique. *Free Radic. Biol. Med*. 46(2): 119-126. doi: 10.1016/j.freeradbiomed.2008.09.034

15. Forrester, M.T., Thompson, J.W., Foster, M.W., Nogueira, L., Moseley, M.A., Stamler, J.S. (2009b). Proteomic analysis of S-nitrosylation and denitrosylation by resin-assisted capture. *Nat. Biotechnol*. 27(6): 557-559. doi: 10.1038/nbt.1545

16. Foster, M.W., McMahon, T.J., Stamler, J.S. (2003). S-nitrosylation in Health and Disease. *Cell Press* 9(4): 160-168. doi: 10.1016/s1471-4914(03)00028-5

17. Gandra, P.G., Hogan, M.C., Nogueira, L. (2012). Mitochondrial activation at the onset of contractions in isolated myofibres during successive contractile periods. *J. Physiol.* 1;590(15): 3597-609. doi: 10.1113/jphysiol.2012.232405

18. Gandra, P.G., Shiah, A.A., Nogueira, L., & Hogan, M.C. (2018). A mitochondrial-targeted antioxidant improves myofilament Ca^{2+} sensitivity during prolonged low frequency force depression at low P_{O2}. *J. Physiol.* 596(6): 1079–1089. doi: https://doi.org/10.1113/JP275470

19. Green, H.J. (1997). Mechanisms of muscle fatigue in intense exercise. *Jour. Sports Sci.* 15(3): 247-256. doi: 10.1080/026404197367254

20. Griffith, O.W., Kilbourn, R.G. (1996). Nitric oxide synthase inhibitors: amino acids. *Methods Enzymol*. 268: doi: 375-392. doi:10.1016/s0076-6879(96)68040-9

21. Hess, D.T., Matsumoto, A., Kim, S.O., Marshall, H.E., Stamler, J.S. (2005). Protein S-nitrosylation: purview and parameters. *Nat. Rev. Mol. Cell. Biol.* 6(2): 150-166. doi: 10.1038/nrm1569

22. Heunks, L.M., Machiels, H.A., Dekhuijzen, P.N., Prakash, Y.S., Sieck, G.C. (1985). Nitric oxide affects sarcoplasmic calcium release in skeletal myotubes. *J. Appl. Physiol.* 91(5): 2117-24. doi: 10.1152/jappl.2001.91.5.2117.

23. Hogg, N. (2002). The Biochemistry and Physiology of S-Nitrosothiols. *Annu. Rev. Pharm. Tox.* 2002(42): 585-600. doi: 10.1146/annurev.pharmtox.42.092501.104328

24. Jaffrey, S.R., and Snyder, S.H. (2001). The Biotin Switch Method for the Detection of *S*-Nitrosylated Proteins. *Science's STKE,* 2001(86). doi: 10.1126/stke.2001.86.pl1

25. Jensen, D.E., Belka, G.K., du Bois, G.C. (1998). S-Nitrosoglutathione is a substrate for rat alcohol dehydrogenase class III isoenzyme. *Biochem. J.* 331 (Pt 2): 659-668. doi: 10.1042/bj3310659

26. Keller-Ross, M.L., Larson, M., Johnson, B.D. (2019). Skeletal Muscle Fatigability in Heart Failure. *Front. Physiol.* 10: 129. doi: 10.3389/fphys.2019.00129

27. Kim, H.C., Mofarrahi, M., Hussain, S.N.A. (2008). Skeletal muscle dysfunction in patients with chronic obstructive pulmonary disease. *Int. J. Chron. Obstruct. Pulmon. Dis.* 2008;3(4):637-658. doi: 10.2147/copd.s4480

28. Krans, J. (2010). The Sliding Filament Theory of Muscle Contraction. *Nature Edu.* 3(9): 66.

29. Melkonian, E.A., Schury, M.P. (2020). Biochemistry, Anaerobic Glycolysis. *StatPearls Pub.* PMID: 31536301

30. Moon, Y., Cao, Y., Zhu, J., Xu, Y., Balkan, W., Buys, E.S., Diaz, F., Kerrick, G., Hare, J.M., Percival, J.M. (2017). GSNOR Deficiency Enhances *In Situ* Skeletal Muscle Strength, Fatigue Resistance, and RyR1 S-Nitrosylation Without Impacting Mitochondrial Content and Activity. *Antioxid. Redox Signal.* 26(4): 165-181. doi: 10.1089/ars.2015.6548

31. Mukund, K., and Subramaniam, S. (2020). Skeletal muscle: A review of molecular structure and function, in health and disease. *Wiley Interdiscip. Rev. Syst. Biol. Med.* 12(1): e1462. doi: 10.1002/wsbm.1462

32. Nogueira, L., Figueiredo-Freidas, C., Casimiro-Lopes, G., Magdesian, M.H., Assreuy, J., Sorenson, M.M. (2009). Myosin is reversibly inhibited by S-nitrosylation. *Biochem J.* 11, 424(2): 221-231. doi: 10.1042/BJ20091144

33. Nogueira L., Trisko B.M., Lima-Rosa F.L., Jackson, J., Lund-Palau, H., Yamaguchi, M., Breen, E.C. (2018). Cigarette smoke directly impairs skeletal muscle function through capillary regression and altered myofibre calcium kinetics in mice. *J. Physiol*. 596(14): 2901-2916. doi:10.1113/JP275888

34. Piazza, M., Futrega, K., Spratt, D.E., Dieckmann, T., Guillemette, J.G. (2012). Structure and dynamics of calmodulin (CaM) bound to nitric oxide synthase peptides: Effects of a phosphomimetic CaM mutation. *Biochemistry* 51, (17)3651-3661. doi: https://doi.org/10.1021/bi300327z

35. Squire, J.M. (2016). Muscle contraction: Sliding filament history, sarcomere dynamics and the two Huxleys. *Glob. Cardiol. Sci. Pract.* 2016(2):e201611. doi: 10.21542/gcsp.2016.11

36. Stamler, J.S., Meissner, G. (2001). Physiology of Nitric Oxide in Skeletal Muscle. *Phys. Rev.* 2001(81): 209-237. doi: 10.1152/physrev.2001.81.1.209

37. Tengan, C., Rodrigues, G.S., Godinho, R.O. (2012). Nitric Oxide in Skeletal Muscle: Role on Mitochondrial Biogenesis and Function. *Int. J. Mol. Sci.* 13, 17160-17184. doi: 10.3390/ijms131217160

38. Wan, J.J., Qin, Z., Wang, P., Sun, Y., Liu, X. (2017). Muscle fatigue: general understanding and treatment. *Exp. & Mol. Med.* 49, e384. doi: 10.1038/emm.2017.194

39. Zoll, J., N'Guessan, B., Ribera, F., Lampert, E., Bigard, X., Serrurier, B., Fortin, D., Geny, B., Veksler, V., Ventura-Clapier, R., Mettauer, B. (2002). Physical activity changes the regulation of mitochondrial respiration in human skeletal muscle. *J. Physiol.* 543(Pt 1): 191-200. doi: 10.1113/jphysiol.2002.019661